Biol Trace Elem Res (2017) 175:428–439
DOI 10.1007/s12011-016-0789-x

L-Ascorbic Acid Protected Against Extrinsic and Intrinsic Apoptosis Induced by Cobalt Nanoparticles Through ROS Attenuation

Yake Liu[1] · Hongxiang Hong[2] · Xu Lu[3] · Wei Wang[2] · Fan Liu[2] · Huilin Yang[4]

Received: 15 March 2016 / Accepted: 21 June 2016 / Published online: 5 July 2016

Abstract Currently, tissue damage induced by cobalt nanoparticles (CoNPs) and cobalt ions (Co^{2+}) are the most serious syndrome in the patients with metal-on-metal hip prostheses. Therefore, an urgent need exists for the identification of the mechanisms and the development of therapeutic strategies to limit it. The purpose of this study was to explore the mechanism of this damage and to demonstrate if L-ascorbic acid (L-AA) could protect against the cell toxicities induced by CoNPs and Co^{2+} in vitro. With CoNPs and Co^{2+} treatment, cell viability was significantly decreased; the ROS (reactive oxygen species) level in mitochondria was dramatically increased in CoNPs treated cells, but cobalt ions could barely induce the ROS. Consistently, the level of cell apoptosis was increased with the upregulation of pro-apoptotic factors (caspases 8, 9, and 3, and Bax) and the downregulation of anti-apoptotic factor Bcl-2. Besides that, the levels of cytochrome *c* and AIF were increased and released from mitochondria into the cytoplasm. After the cells were pretreated with L-AA, the cell viability decreased by CoNPs was reversed and the ROS induced by CoNPs was suppressed. The level of cell apoptosis induced by CoNPs was decreased as well. But it could not reverse the effects induced by Co^{2+}. These studies demonstrated that CoNPs induce extrinsic and intrinsic apoptotic pathways via generation of ROS, and L-AA could prevent the cytotoxicity by reducing the level of ROS. While Co^{2+} may induce cytotoxicity through other signals, it could not be protected by L-AA treatment.

Keywords Cobalt nanoparticles · Cobalt ions · Oxidative stress · Apoptosis · L-Ascorbic acid

Abbreviations

CoNPs	Cobalt nanoparticles
Co^{2+}	Cobalt ions
TEM	Transmission electron microscopy
SEM	Scanning electron microscope
MOM	Metal-on-metal
L-AA	L-Ascorbic acid
ROS	Reactive oxygen species
Caspase	Cysteinyl aspartate specific proteinase
IARC	International Agency for Research on Cancer
GSH	Glutathione

Introduction

Application of metal-on-metal (MoM) hip arthroplasty is associated with adverse effects including local soft-tissue reactions and pseudotumors [1]. The MoM hip arthroplasty implants, made of cobalt-chromium (CoCr) alloy, release large amounts of metal nanoparticles and ions in vivo [2]. Commercially available MoM hip arthroplasty implants contain 62 % cobalt (Co) and 28 % chromium (Cr), yielding a Co/Cr ratio of 2.21 [3]. CoNPs are one of the most important degradation products of MoM implants [4]. Therefore, cobalt may be potentially toxic in MoM implants.

Yake Liu and Hongxiang Hong contributed equally to this work.

✉ Huilin Yang
yanghuilin914@163.com

[1] First Affiliated Hospital of Soochow University, Suzhou, Jiangsu Province, People's Republic of China

[2] Department of Orthopedics, The Affiliated Hospital to Nantong University, Nantong, Jiangsu Province, People's Republic of China

[3] Department of Pharmacology, School of Pharmacy, Nantong University, Nantong, Jiangsu Province, People's Republic of China

[4] Department of Orthopedics, The First Affiliated Hospital to Soochow University, Shizi Street, Suzhou 215006, Jiangsu Province, People's Republic of China

In vitro studies demonstrated cobalt caused cell oxidative stress [5], DNA damage [6], inflammatory responses, and genotoxic effects [7]. Furthermore, the International Agency for Research on Cancer (IARC) has classified implanted metallic cobalt as class 2B, "possibly carcinogenic to humans" [8]. Our previous study also demonstrated that exposure to CoNPs and Co^{2+} induced cytotoxicity and genotoxicity in primary human T cells in vitro [9]. Although several experiments suggested significant cytotoxic effects were caused by CoNPs and Co^{2+} treatment, the mechanism of nanomaterial-induced cytotoxicity still has not been clarified yet.

Apoptosis plays an important role in metal toxicity [1]. Although a number of known or suspected human carcinogenic metallic compounds have been shown to induce apoptosis, the relevance of these observations and the carcinogenic process is still unclear [10]. Apoptosis induced by tungsten carbide-Co (WC-Co) fine particles has been reported in vitro [10, 11]. However, apoptotic pathways induced by CoNPs and Co^{2+} are still elusive. Compared with fine particles, WC-Co nanoparticles generated a higher level of ROS and caused more oxidative stress, as evidenced by a decrease in glutathione (GSH) levels [12]. Further studies indicated that catalase, which largely quenched ROS, inhibited WC-Co particle-induced mitochondrial membrane permeability damage in JB6 cells [13]. These results demonstrated that oxidative stress plays an important role in the toxicities induced by WC-Co particles, but the effect on cobalt nanoparticles is still not clarified and needs to be demonstrated.

Along with the exposure to debris from MoM hip prostheses, nano-sized cobalt particles are released and would trigger a series of biochemical reactions. Currently, it is not clear whether CoNPs per se or solubilized Co^{2+} plays a greater role in cytotoxicity. Evidences derived from biochemistry studies involving other nanoparticles in vitro exposure, such as Balb/3T3 cells, suggested that the nanoparticulate fraction was more poisonous than the ionic form [14]. Nanoparticles generated from MoM hip prostheses, including CoCr alloy nanoparticles with an average size of 29.5 ± 6.3 nm, caused greater cell toxicity than the micron-sized particles [15].

In this study, we explored the mechanisms of cytotoxicity of CoNPs together with Co^{2+} and developed strategies to reduce this cytotoxicity with L-AA treatment. The experimental study is focused on CoNPs with an average size of 30 nm and used Co^{2+} to identify the role of Co, without the addition of Cr, in the adverse reactions. Balb/3T3 mouse fibroblast cells were used in toxicity assays in vitro and are approved by the European Centre of Validation of Alternative Methods (ECVAM) [16]. L-Ascorbic acid (L-AA), an antioxidant, was used to reduce the level of oxidative stress. It has been demonstrated that the addition of physiological levels of L-AA decreased the levels of ROS and cytotoxicity induced by CoNPs and Co^{2+}, respectively [17]. We hypothesized that the intrinsic apoptotic pathway was triggered by ROS during exposure to CoNPs in Balb/3T3 cells and contributed to tissue damages in susceptible individuals following MoM hip replacement. The effects of CoNPs compared with Co^{2+} in Balb/3T3 cells were also observed in this study. Furthermore, for the first time, we used L-AA to alter or reduce the toxicity induced by CoNPs and Co^{2+} in Balb/3T3 cells.

Materials and Methods

Materials

Dulbecco's modified Eagle's medium (DMEM), phosphate-buffered saline (PBS), Hank's balanced salt solution (GIBCO® HBSS), and fetal bovine serum (FBS) were purchased from Gibco Invitrogen (Wilmington, MA, USA). Cobalt chloride (Co^{2+}), CoNPs (median size 30 nm), trypsin-EDTA, the penicillin-streptomycin solution, LDH assay kit (MAK066), and MTT (3-(4, 5-dimethylthiazol-2-yl)-2, 5-diphenyltetrazolium bromide) assay kit (TOX1) were obtained from Sigma-Aldrich (St. Louis, MO, USA). GSH, TRIzol-A^+, and reverse transcriptase reaction kit were procured from Nanjing Jiancheng Bioengineering Institute (Nanjing, China). SYBR Green Real-time PCR Master Mix, Cytochrome-C ELISA kit was purchased from Shanghai Yanjin Biological (Shanghai, China). Antibodies against caspase 3, caspase 8, caspase 9, Bax, Bcl-2, AIF, HO-1, and β-actin were obtained from Cell Signaling Technology (Danvers, MA, USA).

Preparation of Co^{2+} and CoNPs

Co^{2+} was suspended in ultrapure water at a concentration of 50 mM, using a 0.22-μm filter to sterilize and store in a deep-freeze for reserve. CoNPs were weighed the day before the experiment, sterilized at 180 °C for 4 h, suspended in ultrapure water at a concentration of 50 mM, sonicated for 15 min with ultrasonic oscillators to disperse CoNPs suspension, and immediately diluted in incomplete culture media (DMEM only). Based on other studies and our pilot experiments, the concentrations of Co^{2+} and CoNPs ranging from 1 to 500 μM were picked up.

Cell Culture

Balb/3T3 mouse fibroblast cells were purchased from ATCC (Manassas, VA) and grown in DMEM supplemented with 10 % FBS, penicillin (100 U/mL), and streptomycin (100 g/mL). The medium was replaced every 3 days. All cells were grown at 37 °C in a humidified incubator containing 5 % CO_2.

Characterization of Cobalt Nanoparticles

CoNPs were characterized for size, shape, and hydrodynamic diameter. The size, microstructure, and elemental composition of CoNPs were assessed by high-resolution scanning electron microscopy (Hitachi 550 ultra high resolution SEM), transmission electron microscopy (TEM, JEM-2100F, Japan), and x-ray diffraction (XRD). In brief, CoNPs were suspended in DMEM supplemented with 5 % FBS at a concentration of 1 mg/mL (pH 7.2–7.4), then the sample was sonicated by using a sonicator bath until a homogeneous suspension formed. A drop of aqueous CoNPs suspension was placed onto a carbon-coated copper grid (300 mesh) and dried in air to obtain SEM and TEM images. XRD was employed for elemental analysis. Dynamic laser light scattering (DLS) measurements were used to determine the hydrodynamic diameter and size distribution of CoNPs in the cell culture medium.

Cellular Uptake

Balb/3T3 cells were incubated with CoNPs 50 μM for 24 h, and the morphologies were analyzed by TEM. TEM analysis was conducted by plating Balb/3T3 cells into six-well tissue culture plates at a density of 5×10^6 cells/well. Followed by CoNPs treatment for 24 h, cells were washed with PBS and fixed with 2.5 % glutaraldehyde and 1 % osmium tetroxide for 3 h, and then dehydrated using graded concentrations of ethanol. After infiltration and embedding in epoxy resin at 60 °C for 48 h, ultra-thin sections (thickness 75 nm) were stained with lead citrate and examined by TEM. TEM imaging and measurement were performed on at least 100 CoNPs. The ultra-thin sections were mounted on Cu lacey carbon-coated TEM grids (200 mesh) and imaged.

Ion Release in Medium

The cells were treated with 50 μM CoNPs for 4, 12, 24, 48, and 72 h. The supernatants were collected and centrifuged at 1500×*g* for 15 min to obtain particle-free medium. The Co^{2+} levels were analyzed by inductively coupled plasma-mass spectrometry (ICP-MS; Agilent 7500A Series). Briefly, the medium was digested with 5 mL 16 M nitric acid followed by 2 mL 30 % (*w*/*w*) hydrogen peroxide. The Co^{2+} content in solution was determined using the ICP-MS. Results were expressed as percentage of CoNPs concentrations.

Cell Viability Assays

Cytotoxicity induced by CoNPs and Co^{2+} was assessed by functional impairment of the mitochondria using MTT assay kit following the manufacturer's instructions [18]. Briefly, cells were plated in DMEM with 10 % FBS at a density of 10^4 cells/well in a 96-well plate. After 24 h, the cells were treated with various doses of CoNPs (1, 5, 10, 50, 100, and 500 μM, respectively) or Co^{2+} (5, 10, 50, 100, and 500 μM, respectively) for 12, 24, and 48 h. After incubation, the original culture was dumped. The MTT labeling reagent was diluted to 0.05 mg/mL in DMEM with 10 % FBS, and then added to each well. Followed by 4 h of incubation, the supernatant was discarded. A total of 150 μL DMSO was added to each well, and the solution was mixed using a microplate oscillator for 10 min. The optical density (OD) of the wells was measured at a wavelength of 490 nm. The cytotoxic concentration was calculated.

Protective Role of L-AA

The effect of L-AA in reducing the cytotoxicity of CoNPs and Co^{2+} was assessed by an MTT assay kit and LDH assay kit. The LDH assay was a precise, fast, and simple colorimetric assay for quantifying cytotoxicity based on LDH activity released from damaged cells [19]. The LDH release in the cell culture medium indicated cell membrane damage. Briefly, cells were planted as before in a 96-well plate. After 24 h of growth, cells were either pretreated with or without L-AA (50 μM, 1 h), and followed by CoNPs (50 μM) or Co^{2+} (50 μM) treatment, respectively, for 24 h. Cell culture supernatants were collected from centrifuged culture media for LDH activity analysis. The LDH levels in the supernatants were measured according to the manufacturer's instructions. The results of MTT assay were measured by the above method.

Measurement of Reactive Oxygen Species

Cells were treated with CoNPs (50 μM) or Co^{2+} (50 μM), respectively, for 24 h in the absence and presence of L-AA (50 μM) pretreated for 1 h. ROS levels were measured using the fluorescence staining [2′, 7′-dichlorodihydro-fluorescein diacetate (H_2DCFDA)]. After exposure to nanoparticles, the cells were incubated with H_2DCFDA (10 μM) at 37 °C for 20 min. The cells were then washed twice with Hank's balanced salt solution (HBSS) to wipe off the extracellular DCFH-DA. The cells were observed with confocal laser scanning microscope and fluorescence microplate. The fluorescence was recorded at 488 nm/525 nm (excitation/emission) wavelengths [18].

GSH Measurement

Glutathione (GSH) was determined in the cells with CoNPs and Co^{2+} (50 μM, 24 h) treatment. After exposure, cells were washed three times with PBS, scraped off, suspended in PBS, and centrifuged at 1000×*g*. The cell pellet was homogenized in 5 % 5-sulfosalicylic acid. The suspension was lysed by freezing and thawing twice and, 5 min later, centrifuged at

10,000×*g* for 10 min. GSH in the supernatant was measured by its ability to convert 5,5¢-dithiobis(2-nitrobenzoic acid) into the yellow product 2-nitrobenzoic acid, as described by Rahman et al. [20]. The amount of GSH was expressed as micromoles per liter of protein, quantified by the Bradford method.

Real-Time Polymerase Chain Reaction

After treated with CoNPs (50 μM) or Co^{2+} (50 μM) for 24 h in the absence and presence of L-AA (50 μM) pretreated for 1 h, total RNA was extracted with TRIzol-A^+, and a reverse transcriptase reaction kit was used to transcribe cDNA from 3000 ng of total RNA according to the manufacturer's guidelines [18]. The SYBR Green Real-time PCR Master Mix was used for all reactions, and quantitative real-time PCR was performed with an Applied Biosystems ABI 7500 Real-Time PCR System using reverse-transcribed cDNA as templates. The primer sequences for the target genes were as follows:

Bax,

Sense: 5′-AGGATGCGTCCACCL-AAGL-AA-3′,

Antisense: 5′-CL-AAAGTAGL-AAGAGGGCL-AACCAC-3′;

Bcl-2,

Sense: 5′-CGAGL-AAGL-AAGAGAGL-AATCACAGG-3′,

Antisense: 5′-L-AATCCGTAGGL-AATCCCL-AACC-3′;

GAPDH,

Sense: 5′-TGL-AACGGGL-AAGCTCACTG-3′,

Antisense: 5′-GCTTCACCACCTTCTTGATGTC-3′.

For all reactions, cycling conditions were 10 min at 95 °C, followed by 40 cycles of 95 °C for 30 s, 62 °C for 30 s, and 68 °C for 30 s. At the completion of cycling, melting curve analysis was performed to establish the specificity of the PCR product. Data were analyzed with Applied Biosystems 7500. The expression of each candidate gene was internally normalized using GAPDH. The relative quantitative value was expressed by the $2^{-\Delta\Delta Ct}$ method. Each experiment was performed in duplicate and repeated three times.

Western Blot

Cells were plated at a density of 4×10^5 cells/well in six-well plates and incubated for 24 h at 37 °C. Then the cells were treated with CoNPs (50 μM) or Co^{2+} (50 μM) for 24 h in the absence and presence of L-AA (50 μM) pretreated for 1 h. After treatment, cells were washed twice with cold PBS, lysed on ice for 30 min in lysis buffer (50 mM Tris-HCl pH 7.4, 1 mM EDTA, 100 mM NaCl, 20 mM NaF, 3 mM Na_3VO_4, and 1 mM PMSF, with 1 % (*v*/*v*) NP-40 and protease inhibitor cocktail). The lysates were centrifuged at 12,000×*g* for 15 min, and the supernatants were recovered. Protein concentrations were determined using the bicinchoninic acid method. After denaturation, 50 μg protein was separated on a 4–12 % Bis Tris gel (Invitrogen) and transferred to a nitrocellulose membrane, and probed with the appropriate primary antibodies overnight at 4 °C. Membrane-bound primary antibodies were detected using the appropriate secondary antibodies. Immunoblots for expression of caspase 9 (#9508), caspase 8 (#4927), and caspase 3 (#9662), Bax (D3R2M), Bcl-2 (D17C4), AIF (D39D2), HO-1 (#70,081), and β-actin (#3700) were detected. All the antibodies were obtained from Cell Signaling Technology (Danvers, MA, USA). Experiments were performed three times, and equal loading of protein was ensured by measuring β-actin expression.

Cytochrome-C ELISA Kit

Double antibody sandwich method was used to measure cytochrome *c*. The microtiter plate was coated with purified mouse cytochrome *c* antibody. The cytochrome *c* and HRP-labeled cytochrome *c* antibody were successively added to the microtiter plate resulting in an antibody-antigen-enzyme-labeled antibody complex. After washing completely, chromogenic substrate TMB was added. The absorbance (OD) was recorded at 450 nm, and the concentration of cytochrome *c* was calculated by comparing with standard curve. Samples were processing according to the manufacture's guidelines.

Statistical Analysis

Data were expressed as mean ± SD (standard deviation) of three independent experiments performed in triplicates. Statistical analysis of the data was performed using one-way analysis of variance (ANOVA), followed by Dunnet's test to evaluate significance relative to control. All statistical analyses were performed with SAS 9.1 statistical software (SAS Institute, Cary, NC, USA). A p value less than 0.05 was considered significant.

Results

Characterization of CoNPs

In this study, the physical properties of the CoNPs were characterized by TEM and SEM analyses. A minimum of 500 particles were analyzed. TEM images of CoNPs showed a spherical morphology and the diameter of single particle was approximately 31.5 ± 2.1 nm after suspension by ultrasonic oscillators in DMEM containing 5 % FBS (pH 7.2–7.4) (Fig. 1a). Using SEM analysis, we found that the nanoparticles were almost smooth and spherical uniformly, with a mean size of 28.6 ± 3.2 nm (Fig. 1b), which was consistent with the TEM analysis. XRD analysis was employed for elemental

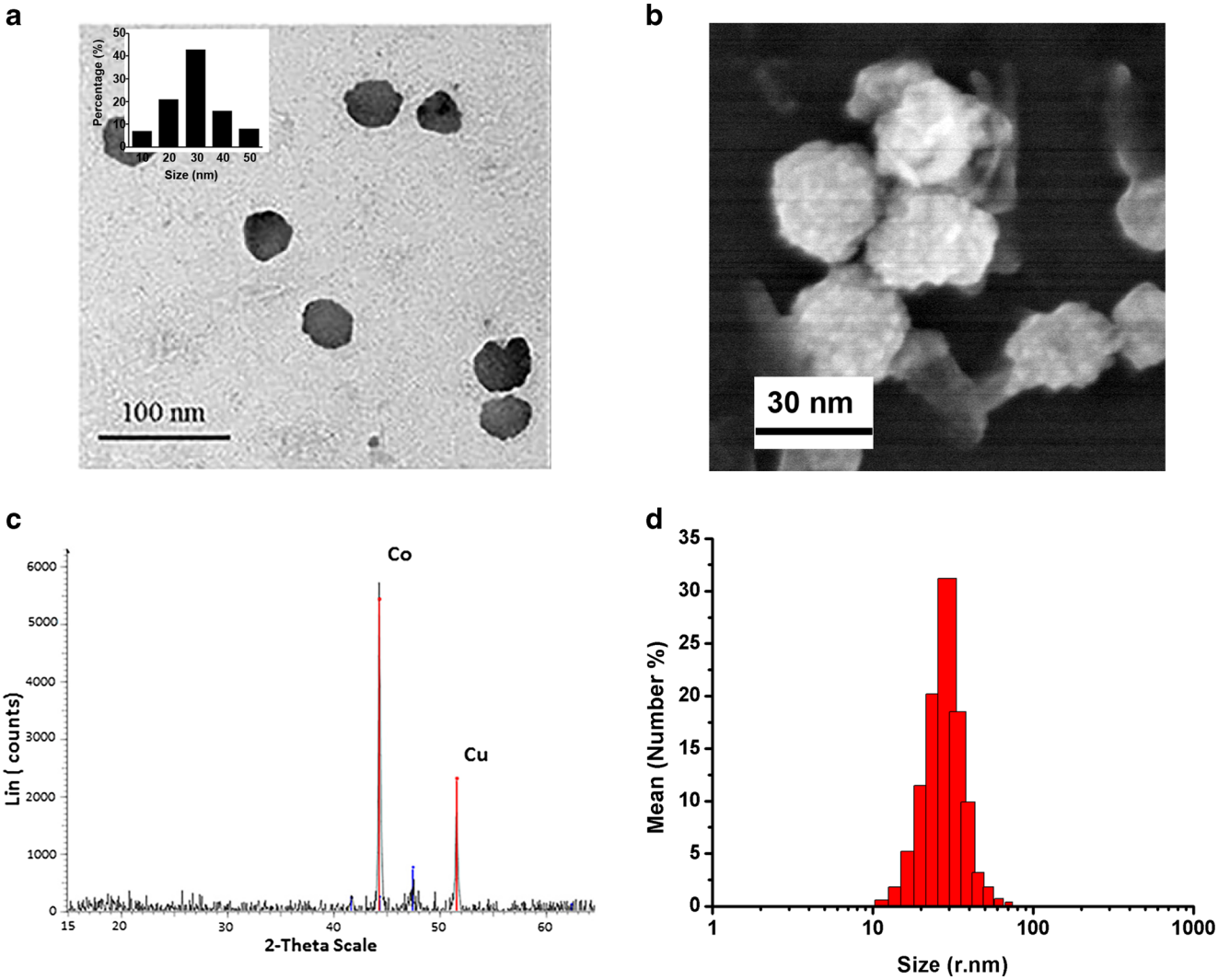

Fig. 1 Characterization of CoNPs. **a** TEM analysis of CoNPs morphology: CoNPs were mainly spherical with a mean diameter of 31.5 ± 2.1 nm (*scale bar* representing 100 nm). The size distribution was obtained by measuring 500 CoNPs. **b** SEM analysis of CoNPs morphology: CoNPs were mainly spherical with a mean diameter of 28.6 ± 3.2 nm (*scale bar* representing 30 nm). **c** XRD analysis was employed for elemental analysis, confirming the presence of Co elements in CoNPs. **d** DLS measurements further confirmed the diameter of CoNPs with a size distribution, which demonstrated that more than 30 % CoNPs was around 30 nm

analysis, confirming the presence of Co elements in CoNPs (Fig. 1c). DLS measurements further confirmed the diameter of CoNPs with a size distribution, which demonstrated that more than 30 % CoNPs was around 30 nm (Fig. 1d).

Cellular Uptake of CoNPs

The uptake of CoNPs by cells is an important factor to assess cytotoxicity and was assessed using TEM analysis after the cells were treated with CoNPs for 24 h (Fig. 2). Compared with non-treatment, there were more cells with nuclear condensation, degenerated mitochondria, and extensive vacuolization with CoNPs treated (Fig. 2a). And the TEM image also revealed that there were many CoNPs in the cells, which indicated that the CoNPs could be uptaken by the cells and induce apoptosis.

Ion Release from CoNPs

The release of Co^{2+} from CoNPs in culture medium was analyzed by ICP-MS after 4, 12, 24, 48, and 72 h of incubation with the indicated doses. A time-dependent increase in the release of Co^{2+} from CoNPs was found with CoNPs treatment ($p < 0.01$) (Fig. 3).

Effects of CoNPs and Co^{2+} on Cell Viability

To determine the cytotoxicity induced by CoNPs and Co^{2+}, Balb/3T3 cells were treated with different doses of either

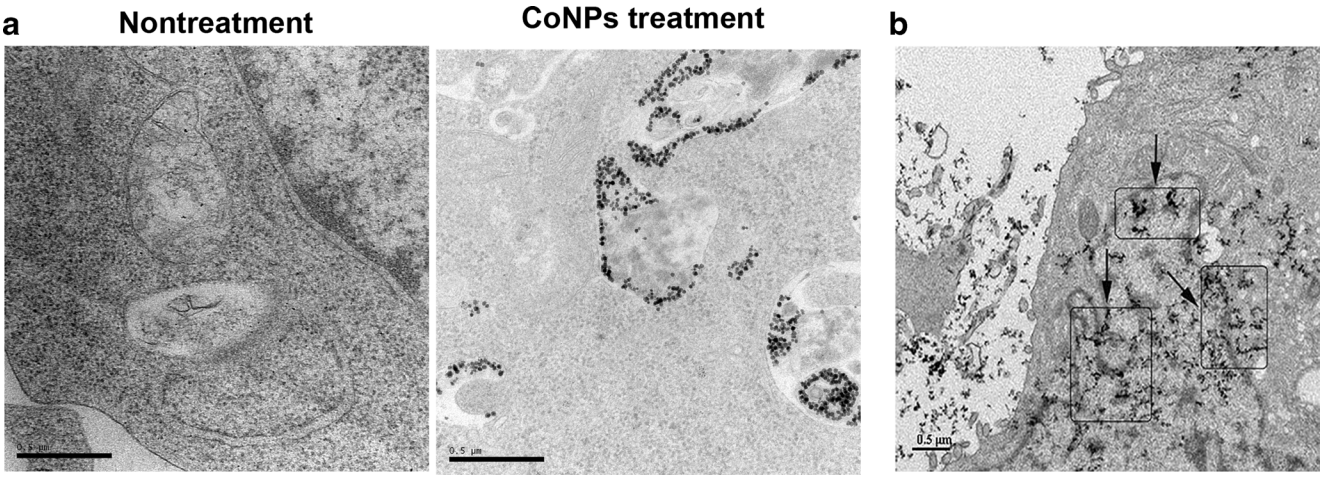

Fig. 2 Cellular uptake of CoNPs. Cells were treated with cobalt nanoparticles (CoNPs 50 μM) for 24 h. **a** TEM analysis reveals that there were more cells with nuclear condensation, mitochondria degeneration, and extensive vacuolization in the cells with CoNPs treatment; **b** TEM images revealed that the CoNPs were uptaken into cytoplasm (indicated by *arrows*)

CoNPs or Co^{2+} (ranged from 1 to 500 μM). After the indicated times (12, 24, and 48 h), MTT assay was used to evaluate the cell viability. CoNPs at 5 μM did not have an obvious influence on cell viability, but a significant reduction of cell viability was induced by CoNPs above 10 μM. However, Co^{2+} inhibited cell viability at concentrations of 50 μM and higher (Fig. 4). The CC50 values at 24 h treated were approximately 50 and 200 μM for CoNPs and Co^{2+}, respectively, which was selected for the subsequent experiments.

L-AA Protected Against CoNPs Induced Cytotoxicity by the Antioxidant Effects

Under oxidative stress, LDH was released from cell membrane, producing biological toxicity. To attenuate the biological toxicity induced by CoNPs, L-ascorbic acid (L-AA), a common antioxidant, was employed. After treated with CoNPs (50 μM) or Co^{2+} (50 μM) in the absence or presence of L-AA (50 μM) for 24 h, the cell viability and biological toxicity were determined by MTT and LDH assays (Fig. 5a, b). In MTT and LDH assays, the viability of the cells treated with Co^{2+} was higher than those treated with CoNPs at the comparable dosage, indicating a higher cytotoxicity of CoNPs treatment. Compared with CoNPs treatment alone, L-AA pretreated for an hour could significantly increase the cell viability ($p < 0.01$), which indicated that the cytotoxicity induced by CoNPs may be caused by oxidative stress. However, pretreatment with L-AA had no effect on the decreased cell viability induced by Co^{2+}.

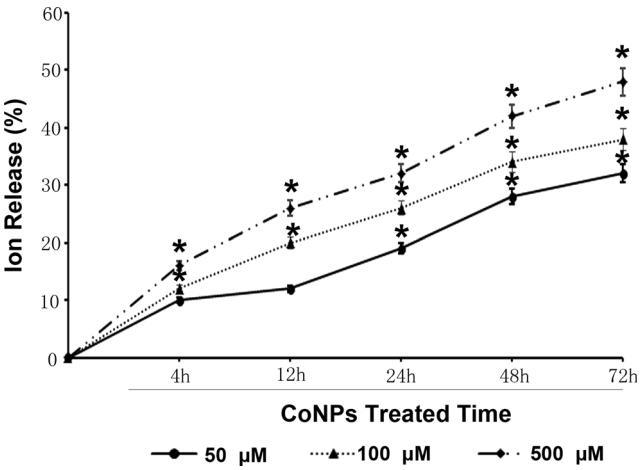

Fig. 3 Ion release from CoNPs. Co^{2+} released from 50 μM of CoNPs after 4, 12, 24, 48, and 72 h of incubation in cell culture medium were measured by ICP-MS. All data were expressed as mean ± SD of three independent experiments performed in triplicates. A linear trend between the Co^{2+} release levels and the exposure time ($p < 0.001$) was observed. *$p < 0.05$, **$p < 0.01$, vs. 4 h group

Effects of CoNPs and Co^{2+} on Cellular ROS, Heme Oxygenase 1 (HO-1), and GSH

Oxidative stress is one of the most important complications induced by nanoparticle exposure [21]. To investigate the level of oxidative stress induced by CoNPs and Co^{2+}, the ROS level was measured. H_2DCFDA, a general ROS sensitive dye, was used to monitor ROS generation induced by CoNPs and Co^{2+} in intact cells. As shown in Fig. 6a and b, ROS levels of cultured cells were significantly increased after 24 h of exposure to 50 μM CoNPs ($p < 0.01$), while L-AA (50 μM) significantly attenuated the increase ($p < 0.01$). Co^{2+} barely increased the ROS level, and L-AA also attenuated the increase mildly.

Since HO-1 is induced by multiple forms of chemical and physical cellular stress; it can represent a general marker of oxidative cellular stress and cytoprotection in oxidative stress [22]. Western blot analysis indicated that CoNPs (50 μM) stimulated HO-1 expression ($p < 0.01$), and L-AA totally inhibited this expression ($p < 0.01$), while Co^{2+} showed no

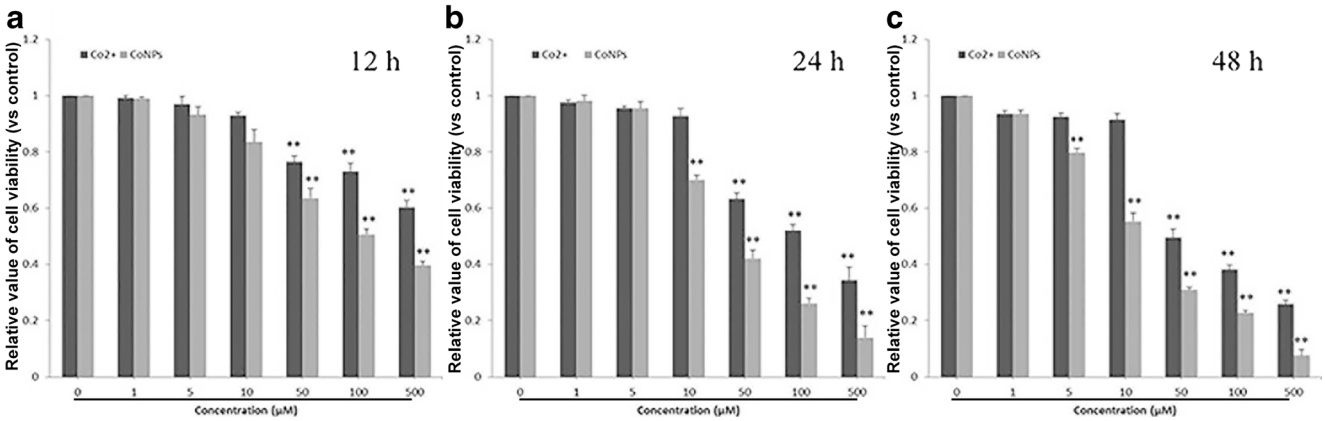

Fig. 4 Cytoxicity analysis in Balb/3T3 cells exposed to CoNPs and Co^{2+}. Cells were treated with CoNPs (0–500 μM) and Co^{2+} (0–500 μM) for 12, 24, and 48 h. All data were expressed as mean ± SD of three independent experiments performed in triplicates. $^{**}p < 0.01$, vs. control

effect on the level of HO-1expression (Fig. 6c). Similarly, GSH is an important antioxidant that protects cells against apoptosis by removing toxic hydrogen peroxide from cells [23]. Further, depletion of GSH appears to promote intracellular ROS accumulation and HO-1 expression, leading to apoptosis [24]. Altered GSH and HO-1 levels represent increased cellular response to oxidative stress. CoNPs treatment decreased GSH levels ($p < 0.01$) and L-AA reversed this decrease ($p < 0.05$) as measured by the GSH assay kit, while Co^{2+} had little effect on GSH (Fig. 6d).

Effects of CoNPs and Co^{2+} on Cytochrome *c* and Apoptosis Inducing Factor (AIF)

To test the effects of CoNPs and Co^{2+} on the intrinsic pathway of apoptosis and the protective effect of L-AA, Balb/3T3 cells were treated with CoNPs (50 μM) or Co^{2+} (50 μM) in the absence or presence of L-AA (50 μM) for 24 h.

ELISA assay revealed that both CoNPs and Co^{2+} caused cytochrome *c* release from mitochondria to cytoplasm ($p < 0.05$), and CoNPs exhibited a greater potency ($p < 0.01$), while L-AA attenuated this release induced by CoNPs ($p < 0.05$) (Fig. 7a).

AIF is a pro-apoptotic factor existing in the mitochondrial intermembrane space [25]. The expression of AIF was examined by Western blot. Upon treatment with CoNPs, the expression of AIF was increased, but L-AA pretreatment attenuated this increase. Also, it is very interesting that L-AA could not suppress the effect induced by Co^{2+} (Fig. 7b).

Effects of CoNPs and Co^{2+} on BAX, Bcl-2, and Caspases 3, 8, and 9

The pro-apoptotic Bax and anti-apoptotic Bcl-2 were detected by Western blot and RT-PCR. In the RT-PCR analysis, the ratio of Bax/Bcl-2 was significantly upregulated by CoNPs

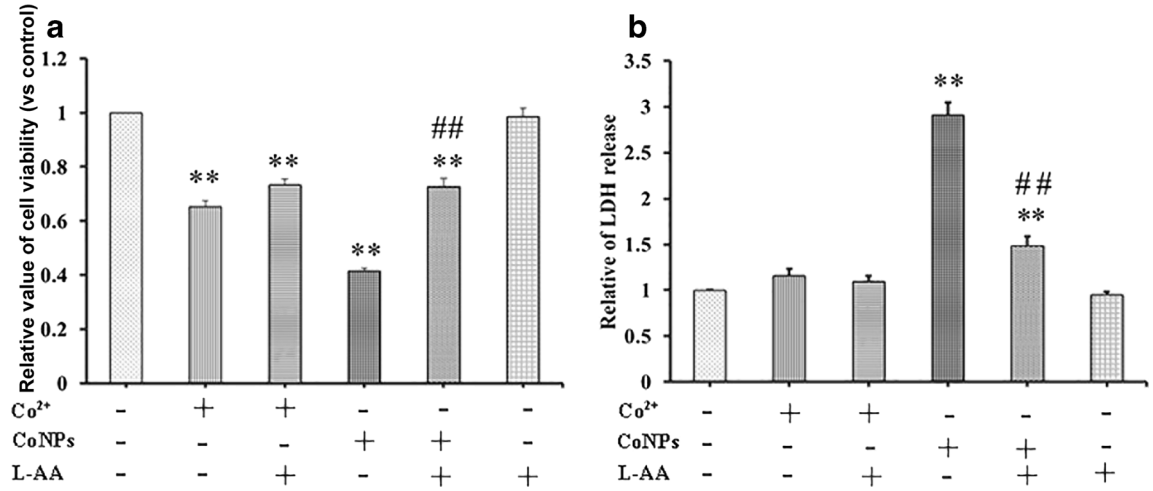

Fig. 5 Protective effect of L-AA on cell viability of Balb/3T3 cells exposed to CoNPs and Co^{2+}. Cells were treated with CoNP (50 μM) or Co^{2+} (50 μM) in the absence or presence of L-AA (50 μM) for 24 h. L-AA pretreatment occurred an hour before CoNPs and Co^{2+}. **a** Data of cells treated with MTT. **b** Data of cells treated with LDH. All data were expressed as mean ± SD of three independent experiments performed in triplicates. $^{*}p < 0.05$, $^{**}p < 0.01$, vs. control. $^{\#\#}p < 0.01$, vs. CoNPs

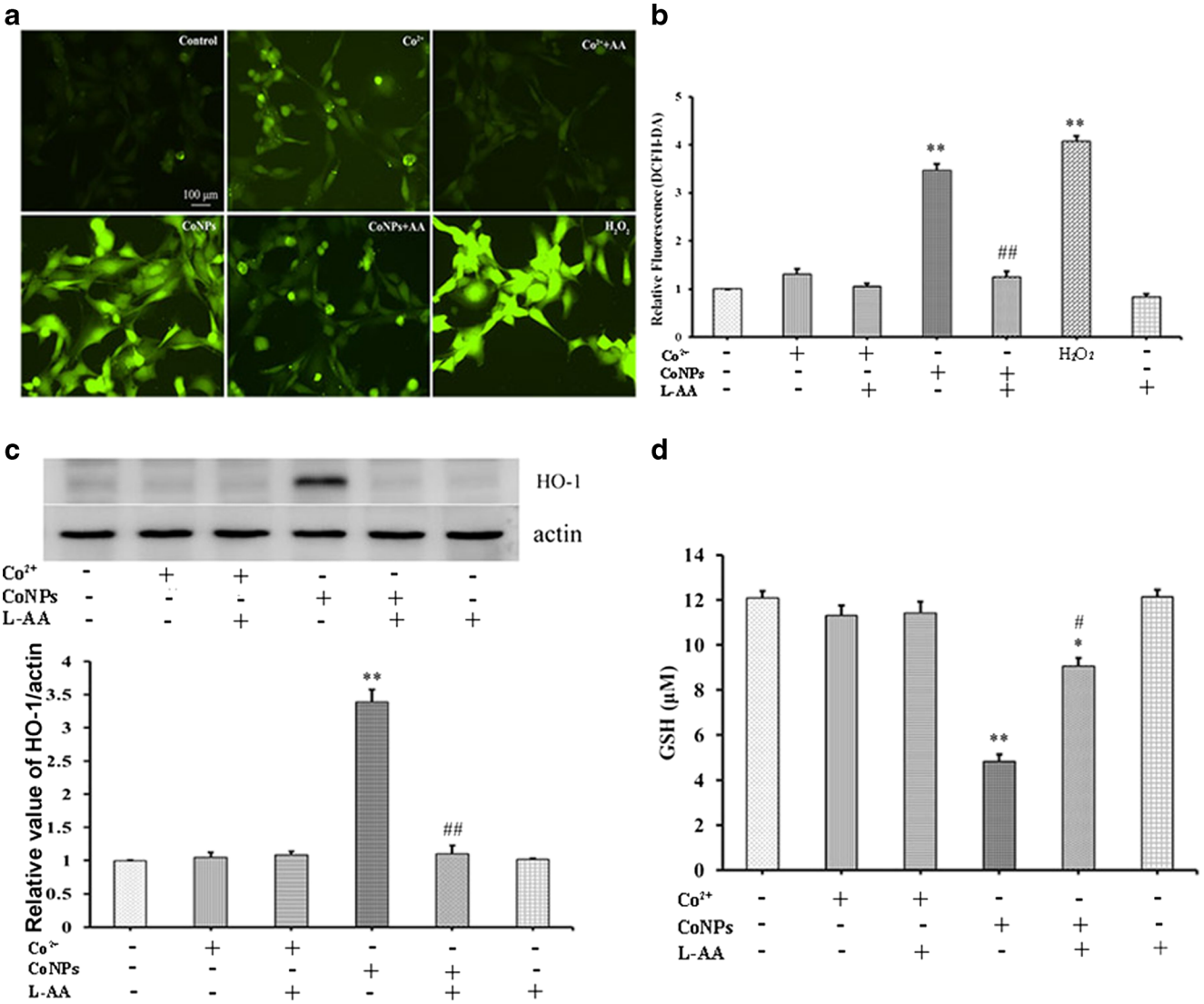

Fig. 6 Effects of CoNPs and Co^{2+} on cellular ROS, HO-1, and GSH. **a**, **b** Generation of cellular ROS in Balb/3T3 cells exposed to CoNPs and Co^{2+}. Cells were grown for 1 day in six-well plates and exposed to CoNPs (50 μM) or Co^{2+} (50 μM) for 24 h with or without L-AA (50 μM) 1 h pretreatment. H_2O_2 (100 μM) was used as a positive control. **a** Cells were visualized with a confocal laser scanning microscope. Each slide was scanned at ×200. The *green color* indicates the fluorescence of detected ROS production. **b** Cells were measured by fluorescence microscopy. All data were expressed as mean ± SD of three independent experiments performed in triplicates. **c** Effects of CoNPs and Co^{2+} on the expression of HO-1. Cells were treated with CoNPs (50 μM) or Co^{2+} (50 μM) in the absence or presence of L-AA (50 μM) for 24 h. L-AA was used for pretreatment 1 h before the addition of CoNPs and Co^{2+}. All data were expressed as mean ± SD of three independent experiments performed in triplicates. **d** Effects of CoNPs and Co^{2+} on GSH. Cells were treated with CoNP (50 μM) or Co^{2+} (50 μM) in the absence or presence of L-AA (50 μM) for 24 h, with L-AA pretreatment 1 h before treatment with CoNPs and Co^{2+}. All data were expressed as mean ± SD of three independent experiments performed in triplicates. $^{**}p < 0.01$, vs. control. $^{\#}p < 0.05$ and $^{\#\#}p < 0.01$, vs. CoNPs

($p < 0.01$) and Co^{2+} ($p < 0.05$), while L-AA attenuated the increase by CoNPs ($p < 0.05$) but had little effect on the Co^{2+}-induced increase (Fig. 8a). Western blots revealed that the expression of Bax was increased by CoNPs and Co^{2+}, while Bcl-2 was significantly decreased, especially by CoNPs. Pretreatment with L-AA, similarly, attenuated the effects of CoNPs, while L-AA had little effect on the Co^{2+}-treated cells (Fig. 8b).

To further confirm the activation of apoptosis, Western blot analysis revealed that caspases 3, 8, and 9 were significantly cleaved when exposed to CoNPs and Co^{2+}, especially when treated with CoNPs. L-AA reduced the cleaved caspase expression induced by CoNPs but not Co^{2+} (Fig. 8b).

Discussion

With the increasing use of MoM hip arthroplasty in orthopedic surgery, metal nanoparticles released from the prosthesis have

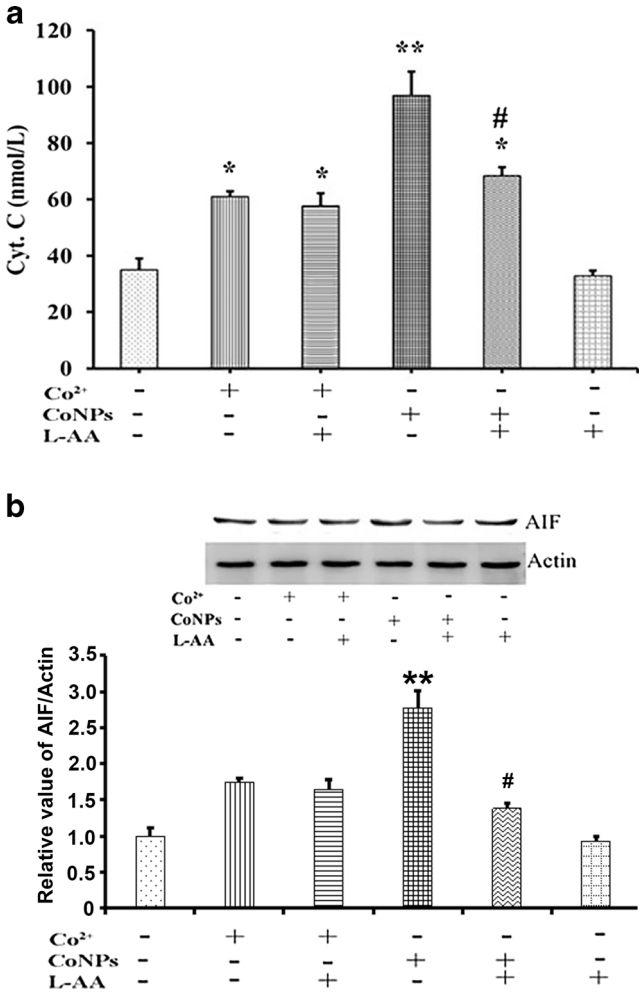

Fig. 7 Effects of CoNPs and Co^{2+} on cytochrome *c* and AIF. **a** Effects of CoNPs and Co^{2+} on cytochrome **c**. Cells were treated with CoNP (50 μM) or Co^{2+} (50 μM) in the absence or presence of L-AA (50 μM) for 24 h. L-AA pretreatment occurred 1 h before treatment with CoNPs and Co^{2+}. The release of cytochrome *c* from mitochondria into cytoplasm was measured by ELISA assay. All data were expressed as mean ± SD of three independent experiments performed in triplicates. **b** Effects of CoNPs and Co^{2+} on the expression of AIF. Cells were treated with CoNP (50 μM) or Co^{2+} (50 μM) in the absence and presence of L-AA (50 μM) for 24 h. L-AA pretreatment occurred 1 h before CoNPs and Co^{2+} treatments. The altered protein levels were determined by Western blot. β-Actin was set as a protein loading control. $*p < 0.05$, $**p < 0.01$, vs. control. $\#p < 0.05$, vs. CoNPs

been recognized as a potential health threat [1]. It has been reported that MoM prostheses cause unexplained pain [26], high blood metal ion levels [27], and early revision rates [28]. In occupational settings, exposure to cobalt leads to various lung diseases, such as interstitial pneumonitis, fibrosis, and asthma [29, 30]. Investigation of periprosthetic tissue showed the presence of metal debris in the form of CoCr nanoparticles and Co as the most likely reactive agent [31, 32]. The toxic effects of CoNPs are likely influenced by their ability to enter cells, leading to corrosion in biological systems [33], which prompted studies of cellular uptake and entry of both nanoparticles and metal ions [34]. However, the molecular mechanisms involved in metal-induced cytotoxicity and the molecular events mediating cellular responses to Co particles remain to be elucidated. In this study, we focused on investigations into the mechanisms of CoNPs and Co^{2+} in the adverse reactions and evaluated the protective effect of L-AA against cobalt-induced cytotoxicity in Balb/3T3 cells in vitro.

Previous studies have demonstrated that CoCr alloy nano-sized particles induced more cell damage than micron-sized particles at equivalent concentrations, suggesting that particle size and surface area may play an important role [15]. Since uptake of CoNPs by cells is closely related to biological behavior, we hypothesized that the uptake of CoNPs by Balb/3T3 cells triggered oxidant stress or cell toxicity. CoNPs gradually dissolve in culture medium and release Co^{2+}, which prompted the question whether the cytotoxic effect was related to particle per se or released ions, or both [35]. ICP-MS was used to measure the ions released from CoNPs. However, under our experimental conditions, the Co^{2+} released from CoNPs was not adequate to induce cell damage. Therefore, the contribution of ions released from CoNPs in DMEM was minimal in inducing cell damage, consistent with our findings in a previous study [9]. In this study, the MTT assay showed that both CoNPs and Co^{2+} induced a decrease in the viability of Balb/3T3 cells. The cytotoxic effects of CoNPs were stronger than Co^{2+}, which indicated that the CoNPs showed higher toxicity than Co^{2+} at similar concentrations. Consistently, LDH leakage to medium due to cell membrane damage indicated irreversible cell death. Pretreatment with L-AA mostly decreased this cytotoxicity, which demonstrated that L-AA protected against Co-induced cytotoxicity through certain protective mechanisms.

Intracellular ROS is a key indicator of various toxic effects associated with nanoparticles [36]. Nanoparticle exposure induces a pro-oxidant environment in the cells, perturbs the redox equilibrium, and leads to adverse biological consequences ranging from early inflammation to relatively large-scale cell death. By measuring ROS, we observed that CoNPs generated a high level of free radicals and induced greater oxidative stress, as evidenced by fluorescence staining, with the decrease of GSH and the increase of HO-1, which played an important role in cellular protection against oxidative stress, hypoxia, or inflammation. The results confirmed the findings of previous studies, which showed that nanoparticles induced toxicity through oxidative stress by generating ROS in cells [37, 38]. Co^{2+} showed no significant increase of ROS. These effects induced by CoNPs were partially prevented by pretreatment with L-AA, an antioxidant precursor of the glutathione deactivating ROS system. However, L-AA had little effect on Co^{2+}, which indicated that the apoptosis induced by CoNPs may correlate with the induction of ROS, and the protective effect of L-AA on cells may be due to the reduction of ROS. Apoptosis is programmed cell death, which is widely

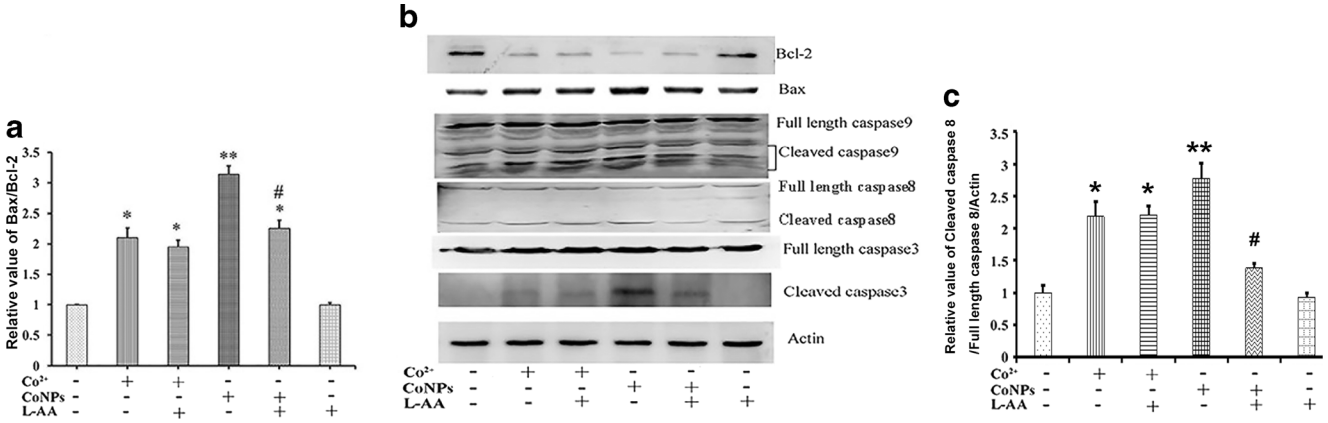

Fig. 8 Effects of CoNPs and Co^{2+} on BAX, Bcl-2, and caspases 3, 8, and 9. **a** Effects of CoNPs and Co^{2+} on mRNA ratio of Bax/Bcl-2. Cells were treated with CoNP (50 μM) or Co^{2+} (50 μM) in the absence and presence of L-AA (50 μM) for 24 h. Pretreatment with L-AA occurred 1 h before CoNPs and Co^{2+} treatments. The expression of Bax and Bcl-2 mRNA was detected by RT-PCR. All data were expressed as mean ± SD of three independent experiments performed in triplicates. **b** Effects of CoNPs and Co^{2+} on the expression of Bcl-2, Bax, and caspases 3, 8, and caspase 9. Cells were treated with CoNPs (50 μM) or Co^{2+} (50 μM) in the absence and presence of L-AA (50 μM) for 24 h, with L-AA 1 h pretreatment. The changes in the protein levels were determined by Western blot. β-Actin was set as a protein loading control. $*p < 0.05$, $**p < 0.01$, vs. control; $\#p < 0.05$, vs. CoNPs

recognized as critically important in health and disease. Although studies have demonstrated that CoNPs and Co^{2+} both induce cell apoptosis [39], the molecular pathways have not been well investigated. In mammals, signaling cascades culminating in apoptotic cell death can be divided into intrinsic or extrinsic pathways. The extrinsic pathway is triggered upon activation of death receptors. In this study, CoNPs and Co^{2+} activated caspase 8, and the effects of CoNPs were stronger than those of Co^{2+}. These results implied that the apoptotic process induced by CoNPs and Co^{2+} may be initiated by the extrinsic signaling pathway. The intrinsic pathway is initiated in mitochondria by oxidative stress and other factors, followed by the release of cytochrome *c* and AIF from mitochondria into the cytoplasm [40]. Our study demonstrated that both CoNPs and Co^{2+} induced the release of cytochrome *c* and AIF from mitochondria to cytoplasm, and CoNPs had a stronger effect. These results suggested the possible induction of the intrinsic apoptotic pathway in cells induced by CoNPs and Co^{2+}.

The mitochondria-mediated intrinsic apoptotic pathway is controlled by Bcl-2 family proteins, which mediates the response to apoptosis. The balance between the pro- and anti-apoptotic proteins of the Bcl-2 family determines cell survival or death [41]. In this study, both CoNPs and Co^{2+} increased the pro-apoptotic factor Bax but decreased the anti-apoptotic factor Bcl-2, especially in CoNPs-treated cells. Addition of L-AA to CoNPs-treated cells attenuated the increase in Bax expression and reversed the decrease of Bcl-2 expression. To further confirm the intrinsic apoptotic pathway activation, mRNA levels of Bax and Bcl-2 were examined by RT-PCR. We found that the ratio of BAX/Bcl-2 mRNA was significantly upregulated when cells were exposed to CoNPs and Co^{2+}, and pretreatment with L-AA attenuated Bax/Bcl-2 transcription induced by CoNPs. Many pro-apoptotic proteins, including cytochrome *c*, AIF, heat shock proteins, Smac/Diablo, and endonuclease G, are released from mitochondria into cytoplasm after alteration in Bax and Bcl-2 levels following pore formation in the mitochondrial membrane and apoptosis [42]. AIF triggers caspase-independent pathways in apoptosis by inducing DNA fragmentation and chromatin condensation [43], while cytochrome *c* induces apoptosis in a caspase-dependent pathway [44]. Therefore, these results suggest that intrinsic apoptosis induced by CoNPs and Co^{2+} in Balb/3T3 cells mediates both caspase-dependent and caspase-independent pathways.

Caspases are a family of cysteine proteases, which play important and essential roles in apoptosis, necrosis, and inflammation. Eleven caspases have been identified in humans. In the present study, CoNPs and Co^{2+} significantly activated caspases 8 and 9, and then activated caspase 3. Administration of L-AA obviously decreased the expression of cleaved caspases 3, 8, and 9 induced by CoNPs. As demonstrated by previous studies, the addition of antioxidants NAC and CsA prevented caspase 3 activation, which supported the hypothesis that apoptosis was triggered by oxidative stress [39]. The novelty of the present study relates to confirming the role of L-AA in protection against both extrinsic and intrinsic apoptosis pathways induced by CoNPs, by decreasing the generation of ROS.

In conclusion, the key findings of this study are as follows: (1) The cytotoxicity and apoptosis induced by CoNPs and Co^{2+} in Balb/3T3 cells were possibly induced via both extrinsic and intrinsic apoptotic pathways, which include upregulation of Bax, caspase 3, 8, and 9, downregulation of Bcl-2, as well as release of AIF and cytochrome *c* from mitochondria into the cytoplasm. Apoptosis induced by CoNPs was probably activated through ROS since L-AA significantly

attenuated the increase in ROS induced by CoNPs. (2) We also demonstrated that L-AA protected against CoNPs-induced cytotoxicity and apoptosis in Balb/3T3 cells by blocking ROS induction. These findings offer novel insights supporting antioxidant therapy as a viable therapeutic option with potential for disease-modifying effects against adverse reactions induced by MoM hip prostheses. (3) The mechanisms of extrinsic and intrinsic apoptotic pathways induced by Co^{2+} need further study. Compared with Co^{2+}, CoNPs induced larger reduction of GSH, increased HO-1 expression, and increased the production of ROS, whereas Co^{2+} did not induce a significant effect on these aspects. Although some studies indicated that Co^{2+} also generated ROS, the opposite conclusions may be attributed to different concentrations and time points and different chemical purities of the Co salt [45]. (4) Although L-AA acid reduced the cytotoxicity induced by CoNPs partially, it could not completely reduce the cytotoxicity induced by CoNPs, suggesting that there may be some other mechanisms of CoNPs-triggered cell toxicity. A previous study reporting silver nanoparticle toxicity demonstrated another pathway induced by cell-cycle inhibition of S-phase leading to anti-proliferative effect, which is a ROS-independent pathway and plays an important role in apoptosis [46]. These two hypotheses still need further investigation.

Acknowledgment This study was funded by the National Natural Science Foundation of China (No. 81171743) and Jiangsu Province Natural Science Foundation of China (No. BK20150399).

Authors' Contributions YKL wrote the manuscript and designed the study, HXH conducted the experimental work and designed the study, XL and WW performed the experimental work and statistical analysis, FL supervised the project and conducted the statistical analysis, and HLY was responsible for the whole project and supervised the study. All authors read and approved the final manuscript.

Compliance with Ethical Standards

Conflict of Interest The authors report no declarations of interest.

References

1. Gill HS, Grammatopoulos G, Adshead S, Tsialogiannis E, Tsiridis E (2012) Molecular and immune toxicity of CoCr nanoparticles in MoM hip arthroplasty. Trends Mol Med 18(3):145–155. doi:10.1016/j.molmed.2011.12.002
2. Xia Z, Kwon YM, Mehmood S, Downing C, Jurkschat K, Murray DW (2011) Characterization of metal-wear nanoparticles in pseudotumor following metal-on-metal hip resurfacing. Nanomed : Nanotechnol Biol Med 7(6):674–681. doi:10.1016/j.nano.2011.08.002
3. Saikko V, Nevalainen J, Revitzer H, Ylinen P (1998) Metal release from total hip articulations in vitro: substantial from CoCr/CoCr, negligible from CoCr/PE and alumina/PE. Acta Orthop Scand 69(5):449–454
4. Milosev I, Remskar M (2009) In vivo production of nanosized metal wear debris formed by tribochemical reaction as confirmed by high-resolution TEM and XPS analyses. J Biomed Mater Res Part A 91(4):1100–1110. doi:10.1002/jbm.a.32301
5. Monteiller C, Tran L, MacNee W, Faux S, Jones A, Miller B, Donaldson K (2007) The pro-inflammatory effects of low-toxicity low-solubility particles, nanoparticles and fine particles, on epithelial cells in vitro: the role of surface area. Occup Environ Med 64(9):609–615. doi:10.1136/oem.2005.024802
6. Ponti J, Sabbioni E, Munaro B, Broggi F, Marmorato P, Franchini F, Colognato R, Rossi F (2009) Genotoxicity and morphological transformation induced by cobalt nanoparticles and cobalt chloride: an in vitro study in Balb/3T3 mouse fibroblasts. Mutagenesis 24(5):439–445. doi:10.1093/mutage/gep027
7. Colognato R, Bonelli A, Ponti J, Farina M, Bergamaschi E, Sabbioni E, Migliore L (2008) Comparative genotoxicity of cobalt nanoparticles and ions on human peripheral leukocytes in vitro. Mutagenesis 23(5):377–382. doi:10.1093/mutage/gen024
8. McGregor DB, Baan RA, Partensky C, Rice JM, Wilbourn JD (2000) Evaluation of the carcinogenic risks to humans associated with surgical implants and other foreign bodies—a report of an IARC monographs Programme meeting. International Agency for Research on Cancer. Eur J Cancer 36(3):307–313
9. Jiang H, Liu F, Yang H, Li Y (2012) Effects of cobalt nanoparticles on human T cells in vitro. Biol Trace Elem Res 146(1):23–29. doi:10.1007/s12011-011-9221-8
10. Lombaert N, De Boeck M, Decordier I, Cundari E, Lison D, Kirsch-Volders M (2004) Evaluation of the apoptogenic potential of hard metal dust (WC-Co), tungsten carbide and metallic cobalt. Toxicol Lett 154(1–2):23–34. doi:10.1016/j.toxlet.2004.06.009
11. Lombaert N, Lison D, Van Hummelen P, Kirsch-Volders M (2008) In vitro expression of hard metal dust (WC-Co)—responsive genes in human peripheral blood mononucleated cells. Toxicol Appl Pharmacol 227(2):299–312. doi:10.1016/j.taap.2007.11.002
12. Ding M, Kisin ER, Zhao J, Bowman L, Lu Y, Jiang B, Leonard S, Vallyathan V, Castranova V, Murray AR, Fadeel B, Shvedova AA (2009) Size-dependent effects of tungsten carbide-cobalt particles on oxygen radical production and activation of cell signaling pathways in murine epidermal cells. Toxicol Appl Pharmacol 241(3):260–268. doi:10.1016/j.taap.2009.09.004
13. Zhao J, Bowman L, Magaye R, Leonard SS, Castranova V, Ding M (2013) Apoptosis induced by tungsten carbide-cobalt nanoparticles in JB6 cells involves ROS generation through both extrinsic and intrinsic apoptosis pathways. Int J Oncol 42(4):1349–1359. doi:10.3892/ijo.2013.1828
14. Sabbioni E, Fortaner S, Farina M, Del Torchio R, Olivato I, Petrarca C, Bernardini G, Mariani-Costantini R, Perconti S, Di Giampaolo L, Gornati R, Di Gioacchino M (2014) Cytotoxicity and morphological transforming potential of cobalt nanoparticles, microparticles and ions in Balb/3T3 mouse fibroblasts: an in vitro model. Nanotoxicology 8(4):455–464. doi:10.3109/17435390.2013.796538
15. Papageorgiou I, Brown C, Schins R, Singh S, Newson R, Davis S, Fisher J, Ingham E, Case CP (2007) The effect of nano- and micron-sized particles of cobalt-chromium alloy on human fibroblasts in vitro. Biomaterials 28(19):2946–2958. doi:10.1016/j.biomaterials.2007.02.034
16. Corvi R, Aardema MJ, Gribaldo L, Hayashi M, Hoffmann S, Schechtman L, Vanparys P (2012) ECVAM prevalidation study on in vitro cell transformation assays: general outline and conclusions of the study. Mutat Res 744(1):12–19. doi:10.1016/j.mrgentox.2011.11.009
17. Nyga A, Hart A, Tetley TD (2015) Importance of the HIF pathway in cobalt nanoparticle-induced cytotoxicity and inflammation in human macrophages. Nanotoxicology 9(7):905–917. doi:10.3109/17435390.2014.991430

18. Tao S, Zheng Y, Lau A, Jaramillo MC, Chau BT, Lantz RC, Wong PK, Wondrak GT, Zhang DD (2013) Tanshinone I activates the Nrf2-dependent antioxidant response and protects against As(III)-induced lung inflammation in vitro and in vivo. Antioxid Redox Signal 19(14):1647–1661. doi:10.1089/ars.2012.5117
19. Nguyen VT, Ko SC, Oh GW, Heo SY, Jeon YJ, Park WS, Choi IW, Choi SW, Jung WK (2016) Anti-inflammatory effects of sodium alginate/gelatine porous scaffolds merged with fucoidan in murine microglial BV2 cells. Int J Biol Macromol. doi:10.1016/j.ijbiomac.2016.05.078
20. Rahman I, Kode A, Biswas SK (2006) Assay for quantitative determination of glutathione and glutathione disulfide levels using enzymatic recycling method. Nat Protoc 1(6):3159–3165. doi:10.1038/nprot.2006.378
21. Nel A, Xia T, Madler L, Li N (2006) Toxic potential of materials at the nanolevel. Science 311(5761):622–627. doi:10.1126/science.1114397
22. Kim HP, Wang X, Chen ZH, Lee SJ, Huang MH, Wang Y, Ryter SW, Choi AM (2008) Autophagic proteins regulate cigarette smoke-induced apoptosis: protective role of heme oxygenase-1. Autophagy 4(7):887–895
23. Paolicchi A, Dominici S, Pieri L, Maellaro E, Pompella A (2002) Glutathione catabolism as a signaling mechanism. Biochem Pharmacol 64(5–6):1027–1035
24. Oguro T, Hayashi M, Nakajo S, Numazawa S, Yoshida T (1998) The expression of heme oxygenase-1 gene responded to oxidative stress produced by phorone, a glutathione depletor, in the rat liver; the relevance to activation of c-Jun n-terminal kinase. J Pharmacol Exp Ther 287(2):773–778
25. Susin SA, Daugas E, Ravagnan L, Samejima K, Zamzami N, Loeffler M, Costantini P, Ferri KF, Irinopoulou T, Prevost MC, Brothers G, Mak TW, Penninger J, Earnshaw WC, Kroemer G (2000) Two distinct pathways leading to nuclear apoptosis. J Exp Med 192(4):571–580
26. Campbell P, Shimmin A, Walter L, Solomon M (2008) Metal sensitivity as a cause of groin pain in metal-on-metal hip resurfacing. J Arthroplast 23(7):1080–1085. doi:10.1016/j.arth.2007.09.024
27. Hart AJ, Skinner JA, Winship P, Faria N, Kulinskaya E, Webster D, Muirhead-Allwood S, Aldam CH, Anwar H, Powell JJ (2009) Circulating levels of cobalt and chromium from metal-on-metal hip replacement are associated with CD8+ T-cell lymphopenia. J Bone Joint Surg Br Vol 91(6):835–842. doi:10.1302/0301-620X.91B6.21844
28. Huang DC, Tatman P, Mehle S, Gioe TJ (2013) Cumulative revision rate is higher in metal-on-metal THA than metal-on-polyethylene THA: analysis of survival in a community registry. Clin Orthop Relat Res 471(6):1920–1925. doi:10.1007/s11999-013-2821-1
29. Cirla AM (1994) Cobalt-related asthma: clinical and immunological aspects. Sci Total Environ 150(1–3):85–94
30. Lison D, Lauwerys R, Demedts M, Nemery B (1996) Experimental research into the pathogenesis of cobalt/hard metal lung disease. Eur Respir J 9(5):1024–1028
31. Hart AJ, Quinn PD, Lali F, Sampson B, Skinner JA, Powell JJ, Nolan J, Tucker K, Donell S, Flanagan A, Mosselmans JF (2012) Cobalt from metal-on-metal hip replacements may be the clinically relevant active agent responsible for periprosthetic tissue reactions. Acta Biomater 8(10):3865–3873. doi:10.1016/j.actbio.2012.05.003
32. Perumal V, Alkire M, Swank ML (2010) Unusual presentation of cobalt hypersensitivity in a patient with a metal-on-metal bearing in total hip arthroplasty. Am J Orthop 39(5):E39–E41
33. Black J (1984) Systemic effects of biomaterials. Biomaterials 5(1):11–18
34. Dillon CT, Lay PA, Bonin AM, Cholewa M, Legge GJ (2000) Permeability, cytotoxicity, and genotoxicity of Cr(III) complexes and some Cr(V) analogues in V79 Chinese hamster lung cells. Chem Res Toxicol 13(8):742–748
35. Papis E, Gornati R, Prati M, Ponti J, Sabbioni E, Bernardini G (2007) Gene expression in nanotoxicology research: analysis by differential display in BALB3T3 fibroblasts exposed to cobalt particles and ions. Toxicol Lett 170(3):185–192. doi:10.1016/j.toxlet.2007.03.005
36. Xia T, Kovochich M, Brant J, Hotze M, Sempf J, Oberley T, Sioutas C, Yeh JI, Wiesner MR, Nel AE (2006) Comparison of the abilities of ambient and manufactured nanoparticles to induce cellular toxicity according to an oxidative stress paradigm. Nano Lett 6(8):1794–1807. doi:10.1021/nl061025k
37. Avalos A, Haza AI, Mateo D, Morales P (2014) Cytotoxicity and ROS production of manufactured silver nanoparticles of different sizes in hepatoma and leukemia cells. J Appl Toxicol : JAT 34(4):413–423. doi:10.1002/jat.2957
38. Park EJ, Yi J, Kim Y, Choi K, Park K (2010) Silver nanoparticles induce cytotoxicity by a Trojan-horse type mechanism. Toxicol In Vitro : Int J Published Assoc BIBRA 24(3):872–878. doi:10.1016/j.tiv.2009.12.001
39. Battaglia V, Compagnone A, Bandino A, Bragadin M, Rossi CA, Zanetti F, Colombatto S, Grillo MA, Toninello A (2009) Cobalt induces oxidative stress in isolated liver mitochondria responsible for permeability transition and intrinsic apoptosis in hepatocyte primary cultures. Int J Biochem Cell Biol 41(3):586–594. doi:10.1016/j.biocel.2008.07.012
40. Caroppi P, Sinibaldi F, Fiorucci L, Santucci R (2009) Apoptosis and human diseases: mitochondrion damage and lethal role of released cytochrome C as proapoptotic protein. Curr Med Chem 16(31):4058–4065
41. Yang W, Shi L, Chen L, Zhang B, Ma K, Liu Y, Qian Y (2014) Protective effects of perindopril on d-galactose and aluminum trichloride induced neurotoxicity via the apoptosis of mitochondria-mediated intrinsic pathway in the hippocampus of mice. Brain Res Bull 109:46–53. doi:10.1016/j.brainresbull.2014.09.010
42. Siskind LJ, Kolesnick RN, Colombini M (2006) Ceramide forms channels in mitochondrial outer membranes at physiologically relevant concentrations. Mitochondrion 6(3):118–125. doi:10.1016/j.mito.2006.03.002
43. Landshamer S, Hoehn M, Barth N, Duvezin-Caubet S, Schwake G, Tobaben S, Kazhdan I, Becattini B, Zahler S, Vollmar A, Pellecchia M, Reichert A, Plesnila N, Wagner E, Culmsee C (2008) Bid-induced release of AIF from mitochondria causes immediate neuronal cell death. Cell Death Differ 15(10):1553–1563. doi:10.1038/cdd.2008.78
44. Garland JM, Rudin C (1998) Cytochrome c induces caspase-dependent apoptosis in intact hematopoietic cells and overrides apoptosis suppression mediated by bcl-2, growth factor signaling, MAP-kinase-kinase, and malignant change. Blood 92(4):1235–1246
45. Nyga A, Hart A, Tetley TD (2015) Importance of the HIF pathway in cobalt nanoparticle-induced cytotoxicity and inflammation in human macrophages. Nanotoxicology:1–13. doi:10.3109/17435390.2014.991430
46. Chairuangkitti P, Lawanprasert S, Roytrakul S, Aueviriyavit S, Phummiratch D, Kulthong K, Chanvorachote P, Maniratanachote R (2013) Silver nanoparticles induce toxicity in A549 cells via ROS-dependent and ROS-independent pathways. Toxicol In Vitro: Int J Published Assoc BIBRA 27(1):330–338. doi:10.1016/j.tiv.2012.08.021